GEOLOGY | THE GEOLOGICAL SOCIETY OF AMERICA®

https://doi.org/10.1130/G45918.1

Manuscript received 21 September 2018
Revised manuscript received 20 December 2018
Manuscript accepted 20 December 2018

Petrological evidence supports the death mask model for the preservation of Ediacaran soft-bodied organisms in South Australia

Alexander G. Liu[1], Sean McMahon[2], Jack J. Matthews[3,4], John W. Still[5], and Alexander T. Brasier[5]
[1]Department of Earth Sciences, University of Cambridge, Cambridge CB2 3EQ, UK
[2]UK Centre for Astrobiology, School of Physics and Astronomy, University of Edinburgh, Edinburgh EH9 3FD, UK
[3]Department of Earth Sciences, Memorial University of Newfoundland, St. John's, NL A1C 3X5, Canada
[4]Oxford University Museum of Natural History, Oxford OX1 3PW, UK
[5]School of Geosciences, University of Aberdeen, King's College, Aberdeen AB24 3UE, UK

ABSTRACT

Microbially mediated early diagenetic pyrite formation in the immediate vicinity of organic material has been the favored mechanism by which to explain widespread preservation of soft-bodied organisms in late Ediacaran sedimentary successions, but an alternative rapid silicification model has been proposed for macrofossil preservation in sandstones of the Ediacara Member in South Australia. We here provide petrological evidence from Nilpena National Heritage Site and Ediacara Conservation Park to demonstrate the presence of grain-coating iron oxides, framboidal hematite, and clay minerals along Ediacara Member sandstone bedding planes, including fossil-bearing bed soles. Scanning electron microscope (SEM), cathodoluminescence microscopy (CL), and petrographic data reveal that framboids and grain coatings, which we interpret as oxidized pyrite, formed before the precipitation of silica cements. In conjunction with geochemical and taphonomic considerations, our data suggest that anactualistically high concentrations of silica need not be invoked to explain Ediacara Member fossil preservation: We conclude that the pyritic death mask model remains compelling.

INTRODUCTION

The taphonomy of the late Ediacaran Ediacara Member, South Australia—a silica-cemented, quartzofeldspathic arenite containing detailed three-dimensional molds and casts of soft-bodied macro-organisms and matgrounds (e.g., Droser et al., 2017; Fig. 1A)—has been the subject of considerable discussion. For almost 20 years, the leading explanation for the preservation of Ediacara Member macrofossils has been the "death mask" model (Gehling, 1999), whereby extensive benthic microbial communities produced sulfides via sulfate reduction during burial, decay, and early diagenesis. These sulfides are predicted to have reacted with iron in the sediment to form iron monosulfides and ultimately pyrite, rapidly mineralizing both the seafloor and the exterior impressions of any interred carcasses (Gehling, 1999). This mechanism is supported by petrological and sedimentological data from multiple late Ediacaran localities and facies (e.g., Gehling et al., 2005; Narbonne, 2005; Liu, 2016), although complementary processes, such as clay mineral replication, kerogenization, adsorption of reduced iron onto organic matter, or pyritization, may have contributed to preservation in some global settings (Laflamme et al., 2011; Schiffbauer et al., 2014; Ivantsov, 2016; MacGabhann et al., 2019).

Tarhan et al. (2016) proposed an alternative taphonomic model for the Ediacara Member, arguing that Ediacara-style exceptional preservation in sandstone, and the restriction of such preservation to the Proterozoic and early Paleozoic, can be explained by the presence of anactualistically high concentrations of marine dissolved silica. Ediacara Member silica cements within wave-base, sheet-flow, and delta-front sandstone facies (the oscillation-rippled, planar-laminated and rip-up, and flat-laminated to linguoid-rippled sandstone facies, respectively, of Tarhan et al., 2017) at Nilpena National Heritage Site record germanium/silicon (Ge/Si) ratios significantly higher than those of adjacent detrital sand grains, and so they could not

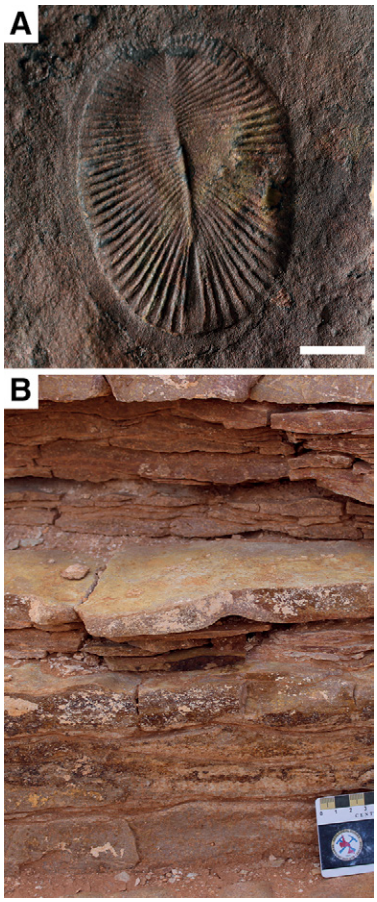

Figure 1. A: Ediacaran macrofossil *Dickinsonia costata* (SAM P51194) from the Ediacara Member of the Rawnsley Quartzite, Nilpena National Heritage Site, South Australia. Scale bar = 10 mm. B: Field photograph of sedimentology within wave-base (oscillation-rippled) sand facies (sensu Gehling and Droser, 2013) at Nilpena.

CITATION: Liu, A.G., et al., 2019, Petrological evidence supports the death mask model for the preservation of Ediacaran soft-bodied organisms in South Australia: Geology, https://doi.org/10.1130/G45918.1

have derived their silica from these grains by metamorphic remobilization. The cements were instead interpreted to reflect preferential nucleation of silica directly from Ediacaran seawater onto microbial mats and organisms shortly after burial, welding the sand grains into coherent molds that were stable enough to retain their relief throughout the collapse and decay of the carcasses. This model noted the paucity of clay or mud laminations between fossil-bearing part and counterpart surfaces (see Tarhan et al., 2017), and it has been supported by uranium isotopic studies that interpret iron-oxide veneers on fossil-bearing surfaces (considered a key line of evidence for original pyrite in the death mask hypothesis; Gehling, 1999) to have been emplaced in the past 2 m.y. (Tarhan et al., 2018). Measured uranium isotope compositions ($^{234}U/^{238}U$) on these iron oxide–coated bed surfaces are far from secular equilibrium (Tarhan et al., 2018), leading those authors to conclude that the oxides were introduced into the sandstones during the Quaternary, precluding use of their presence or distributions as evidence to investigate original or early diagenetic conditions.

The death mask and silicification hypotheses outlined here have distinct and important implications for our understanding of late Ediacaran marine biogeochemistry. The silicification hypothesis implies that silica was concentrated enough in the Ediacaran oceans to precipitate very near the seafloor in subtidal settings, despite known Ediacaran subtidal cherts generally being not primary but replacive after carbonate, and abundant subtidal cherts and silicilytes appearing only across the Ediacaran-Cambrian boundary (postdating deposition of the Ediacara Member; Sievers, 1992; Maliva et al., 2005; Brasier et al., 2011; Perry and Lefticariu, 2014; Dong et al., 2015; Stolper et al., 2017). Conversely, the death mask hypothesis implies that the decay and mineralization of widespread microbial matgrounds could have contributed to the high pyrite burial flux inferred for Ediacaran marine sediments (Liu, 2016; Shields, 2018). The taphonomic models also differ in their predictions regarding the interpretation of fossil morphology (Gibson et al., 2018). We examined thin sections through South Australian fossil-bearing beds in an attempt to distinguish between these two competing models.

METHODS

We studied sedimentary samples representing nine distinct Ediacara Member fossil-bearing levels from Nilpena National Heritage Site (e.g., Fig. 1B) and Greenwood Cliff in Ediacara Conservation Park, South Australia. Figured specimen AU15–2 originated from One Tree Hill, Nilpena, within the oscillation-rippled facies of the Ediacara Member (Droser et al., 2019). Figured specimens AU15–9 and AU15–12 came from North Ediacara Conservation Park close to Greenwood Cliff, in flat-laminated to linguoid-rippled sandstone facies (Coutts et al., 2016; following the terminology of Tarhan et al., 2017). Scanning electron microscope (SEM) analysis of carbon-coated and polished, uncovered thin sections cut perpendicular to bedding through fossil-bearing bed soles (Fig. DR1 in the GSA Data Repository[1]) was undertaken at the Analysis and Characterization facility of the Aberdeen Centre for Electron Microscopy, University of Aberdeen, using a Carl Zeiss GeminiSEM 300 VP equipped with a Deben Centaurus CL detector, an Oxford Instruments NanoAnalysis Xmax80 X-ray energy-dispersive spectrometer (EDS), and the Aztec Energy software suite. An accelerating voltage of 12 kV was used for CL imaging. Raman spectra were acquired with an inVia™ Raman system (Renishaw Plc, UK) coupled to a Leica DM LM microscope at the University of Edinburgh. The 785 nm excitation laser beam (Toptica) was focused onto the samples using a ×100/0.9 NA objective lens (Leica, HCX PL Fluotar), providing an excitation spot of 1 µm diameter. Raman point spectra were taken at different positions on the samples over the range 100–2000 cm^{-1} in extended scan mode. The spectra were acquired with 30 s exposure time using a 600 lines/mm diffraction grating and 8.8 mW excitation power. WiRE™ 2.0 software (https://www.renishaw.com/en/raman-software--9450) was used for data acquisition.

RESULTS

Optical microscopy confirmed the general character of the Ediacara Member fossil-bearing beds as quartzofeldspathic arenites bound by syntaxial silica cements in optical continuity with the host grains, as observed by Tarhan et al. (2016). However, widespread, abundant euhedral microcrystalline iron oxides were observed in direct contact with quartz and feldspar grains on fossil-bearing bed soles, and encased within the silica cement (Figs. 2A–2E). SEM revealed that these iron oxides occur both at the present-day grain boundaries and as "ghosts" recording original sand grain boundaries, embedded fully within silica overgrowths (Figs. 3E and 3F; Fig. DR2). Iron oxides in these two settings are identical in appearance and contiguous in distribution (Figs. DR2C and DR2D). We also identified laminae ≤1 mm thick, characterized by relatively fine sand-sized grains surrounded by abundant grain-coating iron oxides and clay mineral flakes, all within silica cement (Figs. 2B and 2F; Fig. DR3). The clay flakes are oriented plane-parallel to bedding and commonly control the distribution of minor bedding-parallel fractures close to the bed soles. Such clay-rich laminae adhere directly to the hematite-rich bed sole in some samples (Fig. DR3). These laminae are extremely friable and easily lost during weathering, sampling, and sample preparation.

Associated with the iron-oxide primary grain coatings, and also present in small numbers in otherwise pure silica cements, we found discrete spherical structures ~5 to 15 mm in diameter. These manifest as solid brown-red balls in transmitted light, but they were revealed by SEM to comprise framboidal clusters of euhedral, submicron crystals identical to the grain coatings, and, like them, entirely encased within the silica cement (Fig. 3). EDS revealed no evidence of sulfur (Figs. DR4 and DR5), and Raman spectroscopy confirmed that the grain coatings and framboids were composed of hematite (Fig. DR6).

DISCUSSION

Our petrographic observations reveal horizons defined by hematite grain coatings and clusters of hematite framboids within the fossil-bearing beds of the Ediacara Member. These iron oxides, located both at and within a few hundred microns of bed soles (Fig. 3), are fully encased within the silica cements and must therefore predate silicification. Fossiliferous bed soles themselves are hematite-rich (as recognized throughout the Ediacara Member; e.g., Fig. 1A) and can be mantled by thin parting laminations characterized by abundant hematite grain coatings and clay minerals (Fig. DR3). The silica-overgrown hematite "ghost" grain coatings are compositionally and morphologically identical to both the silica-cemented framboids and the hematite at younger grain boundaries. This implies that much (probably the majority) of the observed iron oxide originated as pyrite (though see Wilkin and Barnes, 1997, and references therein), which was subsequently oxidized and preserved more or less in situ with limited redistribution. The iron- and clay-rich partings could also be interpreted as the weathering products of pyritic veneers (e.g., Gehling, 1999).

Taken together, our results are clearly compatible with Gehling's (1999) death mask model, bringing the Ediacara Member into line with other late Ediacaran fossil localities showing evidence for both microbial surfaces and original pyrite and/or its oxidation products (Gehling et al., 2005; Liu, 2016). This global record, which appears to indicate early diagenetic pyritization associated with microbially induced decay of organic matter in the absence of bioturbation, offers an anactualistic mechanism for the relatively high pyrite burial flux required by some Ediacaran biogeochemical models (e.g., Shields, 2018).

[1]GSA Data Repository item 2019077, specimen photographs, and EDS and Raman data, is available online at http://www.geosociety.org/datarepository/2019/, or on request from editing@geosociety.org.

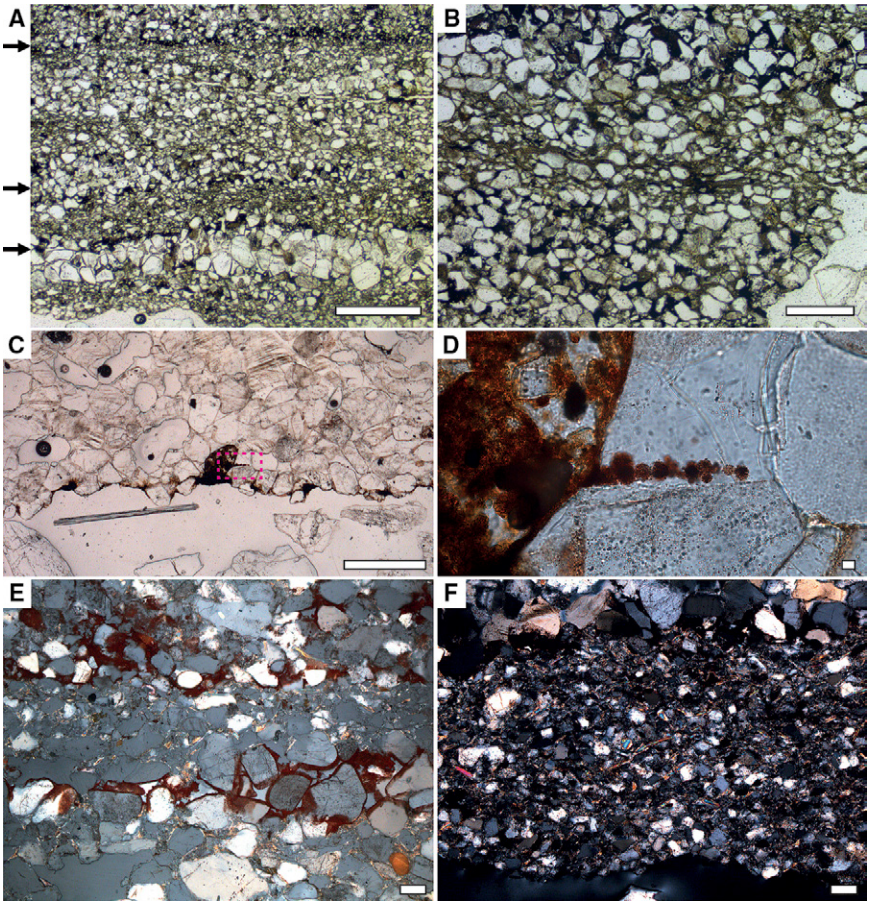

Figure 2. Thin-section photomicrographs showing distribution of framboidal structures and clay minerals in Ediacara Member sandstones, South Australia. A: Thin section of sample AU15–9A in plane-polarized light (ppl), showing thin interbeds of coarse and fine sand, with several iron oxide–rich horizons (arrowed). B: Close-up image of AU15–9A showing abundance of clay minerals in interstices between sand grains in fine-grained laminae. C: Sample AU15–2 in ppl, showing thin iron-oxide veneer on bed sole. D: Close-up of region in box in C, revealing framboidal nature of iron oxides, which appear to be resting on the upper surface of a quartz grain in geopetal fashion, and which are encased in silica. E: Reflected and transmitted light cross-polarized (xpl) view of AU15–9A, showing how red-brown hematite coats quartz grains along discrete horizons, with silica cement infilling spaces after emplacement of iron minerals. F: Xpl view of sample AU15–12, with abundant clay mineral aggregates and detrital muscovite grains picked out by their high birefringence. Scale bars in A and C are 500 µm; in B is 200 µm; in D is 8 µm; in E–F are 80 µm.

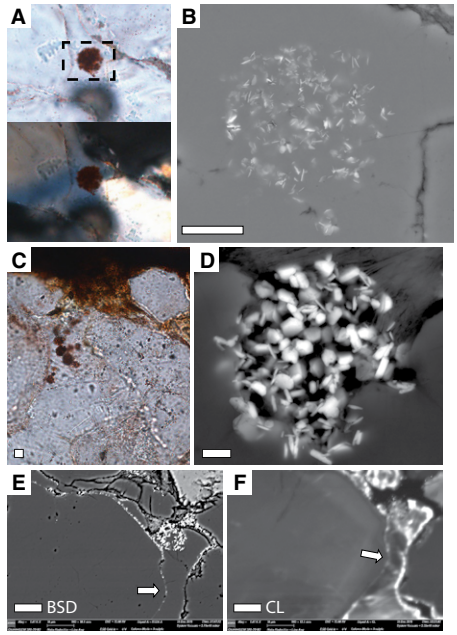

Figure 3. Scanning electron (SEM) and transmitted-light (photo)micrographs showing framboidal microcrystalline iron-oxide aggregates in thin section. A: Photomicrographs of framboids in sample AU15–12. Upper image was taken in plane-polarized light. Lower image, in cross-polarized light, shows that silica cement surrounding the framboid is in optical continuity with grain to left. B: Scanning electron micrograph of boxed area in A; framboid appears smaller because only crystals near surface of silica are visible. Scale bar is 5 µm. C: Photomicrograph showing multiple framboids on surface of quartz grain in sample AU15–2. Bed sole is at top of image. Scale bar is 8 µm. D: Scanning electron micrograph of sample AU15–12, showing framboid with euhedral crystals partly exposed by polishing. E: Backscattered electron diffraction (BSD) image of sample AU15–12 for region at bed sole, showing bands of iron oxides (white) seemingly in the middle of crystals. F: Cathodoluminescence (CL) image of same region in E, revealing that iron oxides are located between two generations of quartz. Iron oxides therefore coat original grains and predate growth of quartz cement. Scale bar in D is 1 µm; in E–F is 10 µm.

In addition to the petrological findings presented here, the silicification model faces other challenges that undermine its credibility as an explanation for Ediacaran taphonomic processes.

First, Ediacara Member silica cements lack the disseminated carbon, clay, and iron minerals that would be expected to have been trapped by the proposed nucleation of early-forming silica directly onto organic mats and carcasses. Such components are not readily lost from within impermeable amorphous/microcrystalline silica: They are pervasive in bona fide early-silica-cemented sandstone-hosted matgrounds as old as 3.2 Ga (e.g., Heubeck, 2009), as well as Precambrian and early Paleozoic cherts and silicilytes (including those cited by Tarhan et al., 2016). The absence of these components in the Ediacara Member silica cements indicates that any original silica cements have been lost, and that the observed cements were emplaced later.

Second, the Ge/Si ratios and petrographic observations central to the argument of Tarhan et al. (2016) may demonstrate that the Ediacara Member silica cements were extraneously sourced, but they do not necessarily indicate an early influx of silica from seawater. The relatively low Ge contents in detrital grains and high Ge contents in silica cements described by those authors are typical of ordinary Phanerozoic sandstones (Götte, 2016). The weak positive correlation between Al and Ge evident in the Ediacara Member cements (Tarhan et al., 2016, their table DR2) is also a familiar feature of Phanerozoic sandstone cements, likely resulting from the comobility of Al and Ge during diagenetic alteration of feldspar and/or kaolinite (Götte, 2016).

We also question the reasoning provided in previous dismissal of the death mask model. Uranium data inferred to demonstrate a recent interaction between Ediacara Member facies and groundwater (Tarhan et al., 2018) do not establish that this interaction redistributed the iron oxides seen on bedding surfaces, or even that the uranium and iron-oxide phases are specifically associated. Moreover, even supposing that the observed iron oxides did form within the past 2 m.y., this finding would in no way undermine the original death mask model, which allows for the late-stage oxidation of early diagenetic iron sulfides when exposed to groundwater. Given the burial and uplift history of Ediacaran sediments in South Australia, it is entirely feasible that the Ediacara Member was only oxidized within the past 2 m.y. Observations of pristine framboidal pyrite veneers on freshly exposed fossil-bearing

Ediacaran surfaces in Newfoundland, Canada (Liu, 2016), alongside iron-oxide staining with patchy surface distributions relating to modern groundwater flow add weight to the suggestion that pyrite can remain unoxidized within Ediacaran-age sedimentary successions until modern exposure. The supposed improbability that iron sulfides could be produced rapidly enough to mold organisms prior to decay (Tarhan et al., 2016) requires experimental testing, and existing experimental data are encouraging (Darroch et al., 2012; Gibson et al., 2018). Similar concerns have been raised regarding whether microcrystalline quartz cementation would be capable of proceeding rapidly enough to act as the primary agent of macrofossil preservation (MacGabhann et al., 2019).

Definitive confirmation of the operation of the death mask model in South Australia awaits the discovery of relict pyrite veneers clearly associated with individual macrofossil specimens. The small size of framboids necessitates undesirable destructive sampling of Ediacara fossils to investigate this. The few relevant studies that claim to bisect Australian Ediacaran fossil material (Retallack, 2016; SI of Tarhan et al., 2016) do not obviously provide images of mineralogy in the immediate vicinity of fossil specimens on bed bases. Until such time as nondestructive microanalysis techniques of sufficient resolution are developed, conclusive demonstration of such thin pyrite veneers without damaging invaluable specimens will be challenging.

Our petrological investigation demonstrates the presence of clusters of hematite framboids, hematite cements directly coating sand grains, and clay minerals in Ediacara Member fossil-bearing sandstones, and indicates that the original iron-mineral cements and framboids predated silica cementation. The death mask and silicification models are not necessarily mutually exclusive—determination of the absolute timing of silica cementation and sulfide formation would be required to conclusively disentangle them—but in light of our observations, we consider the death mask model to remain the most persuasive explanation for macrofossil preservation within the Ediacara Member.

ACKNOWLEDGMENTS

Specimens were collected by Liu with permission and assistance from J. Gehling in 2015. Liu was funded by the Natural Environment Research Council (grant NE/L011409/2). McMahon acknowledges support from the European Union's Horizon 2020 Research and Innovation Programme under Marie Skłodowska-Curie grant agreement 747877, and thanks M. Hall and A. McDonald for help with thin-section polishing and Raman spectroscopy, respectively. Matthews recognizes support from Mitacs (Canada), and all the authors are grateful to N.J. Butterfield for constructive discussions during manuscript preparation. We thank R. Gaines, S. Darroch, and J. Gehling for constructive reviews of this manuscript.

REFERENCES CITED

Brasier, M.D., Antcliffe, J.B., and Callow, R.H.T., 2011, Evolutionary trends in remarkable fossil preservation across the Ediacaran-Cambrian transition and the impact of metazoan mixing, *in* Alison, P.J., and Bottjer, D.J., eds., Taphonomy: Dordrecht, Netherlands, Springer, p. 519–567.

Coutts, F.J., Gehling, J.G., and García-Bellido, D.C., 2016, How diverse were early animal communities? An example from Ediacara Conservation Park, Flinders Ranges, South Australia: Alcheringa, v. 40, p. 407–421, https://doi.org/10.1080/03115518.2016.1206326.

Darroch, S.A., Laflamme, M., Schiffbauer, J.D., and Briggs, D.E., 2012, Experimental formation of a microbial death mask: Palaios, v. 27, p. 293–303, https://doi.org/10.2110/palo.2011.p11-059r.

Dong, L., Shen, B., Lee, C.A., Shu, X., Peng, Y., Sun, Y., Tang, Z., Rong, H., Lang, X., Ma, H., Yang, F., and Guo, W., 2015, Germanium/silicon of the Ediacaran-Cambrian Laobao cherts: Implications for the bedded chert formation and paleoenvironment interpretations: Geochemistry Geophysics Geosystems, v. 16, p. 751–763, https://doi.org/10.1002/2014GC005595.

Droser, M.L., Tarhan, L.G., and Gehling, J.G., 2017, The rise of animals in a changing environment: Global ecological innovation in the late Ediacaran: Annual Review of Earth and Planetary Sciences, v. 45, p. 593–617, https://doi.org/10.1146/annurev-earth-063016-015645.

Droser, M.L., Gehling, J.G., Tarhan, L.G., Evans, S.D., Hall, C.M.S., Hughes, I.V., Hughes, E.B., Dzaugis, M.E., Dzaugis, M.P., Dzaugis, P.W., and Rice, D., 2019, Piecing together the puzzle of the Ediacara biota: Excavation and reconstruction at the Ediacara National Heritage Site Nilpena (South Australia): Palaeogeography, Palaeoclimatology, Palaeoecology, v. 513, p. 132–145, https://doi.org/10.1016/j.palaeo.2017.09.007.

Gehling, J.G., 1999, Microbial mats in terminal Proterozoic siliciclastics; Ediacaran death masks: Palaios, v. 14, p. 40–57, https://doi.org/10.2307/3515360.

Gehling, J.G., and Droser, M.L., 2013, How well do fossil assemblages of the Ediacara biota tell time?: Geology, v. 41, p. 447–450, https://doi.org/10.1130/G33881.1.

Gehling, J.G., Droser, M.L., Jensen, S.R., and Runnegar, B.N., 2005, Ediacara organisms: Relating form to function, *in* Briggs, D.E.G., ed., Evolving Form and Function: Fossils and Development: New Haven, Connecticut, Peabody Museum of Natural History, p. 43–66.

Gibson, B.M., Schiffbauer, J.D., and Darroch, S.A., 2018, Ediacaran-style decay experiments using mollusks and sea anemones: Palaios, v. 33, p. 185–203, https://doi.org/10.2110/palo.2017.091.

Götte, T., 2016, Trace element composition of authigenic quartz in sandstones and its correlation with fluid-rock interaction during diagenesis, *in* Armitage, P.J., et al., eds., Reservoir Quality of Clastic and Carbonate Rocks: Analysis, Modelling and Prediction: Geological Society of London Special Publication 435, p. 373–387, https://doi.org/10.1144/SP435.2.

Heubeck, C., 2009, An early ecosystem of Archean tidal microbial mats (Moodies Group, South Africa, ca. 3.2 Ga): Geology, v. 37, p. 931–934, https://doi.org/10.1130/G30101A.1.

Ivantsov, A.Yu., 2016, Reconstruction of *Charniodiscus yorgensis* (macrobiota from the Vendian of the White Sea): Paleontological Journal, v. 50, p. 1–12, https://doi.org/10.1134/S0031030116010032.

Laflamme, M., Schiffbauer, J.D., Narbonne, G.M., and Briggs, D.E.G., 2011, Microbial biofilms and the preservation of the Ediacara biota: Lethaia, v. 44, p. 203–213, https://doi.org/10.1111/j.1502-3931.2010.00235.x.

Liu, A.G., 2016, Framboidal pyrite shroud confirms the 'death mask' model for moldic preservation of Ediacaran soft-bodied organisms: Palaios, v. 31, p. 259–274, https://doi.org/10.2110/palo.2015.095.

MacGabhann, B.A., Schiffbauer, J.D., Hagadorn, J.W., Van Roy, P., Lynch, E.P., Morrison, L., and Murray, J., 2019, Resolution of the earliest metazoan record: Differential taphonomy of Ediacaran and Paleozoic fossil molds and casts: Palaeogeography, Palaeoclimatology, Palaeoecology, v. 513, p. 146–165, https://doi.org/10.1016/j.palaeo.2018.11.009.

Maliva, R.G., Knoll, A.H., and Simonson, B.M., 2005, Secular change in the Precambrian silica cycle: Insights from chert petrology: Geological Society of America Bulletin, v. 117, p. 835–845, https://doi.org/10.1130/B25555.1.

Narbonne, G.M., 2005, The Ediacara biota: Neoproterozoic origin of animals and their ecosystems: Annual Review of Earth and Planetary Sciences, v. 33, p. 421–442, https://doi.org/10.1146/annurev.earth.33.092203.122519.

Perry, E.C., Jr., and Lefticariu, L., 2014, Formation and geochemistry of Precambrian cherts, *in* Turekian, H.D.H.K., ed., Treatise on Geochemistry (Second Edition), Volume 9: Oxford, UK, Elsevier, p. 113–139, https://doi.org/10.1016/B978-0-08-095975-7.00705-1.

Retallack, G.J., 2016, Ediacaran fossils in thin-section: Alcheringa, v. 40, p. 583–600, https://doi.org/10.1080/03115518.2016.1159412.

Schiffbauer, J.D., Xiao, S., Cai, Y., Wallace, A.F., Hua, H., Hunter, J., Xu, H., Peng, Y., and Kaufman, A.J., 2014, A unifying model for Neoproterozoic–Palaeozoic exceptional fossil preservation through pyritization and carbonaceous compression: Nature Communications, v. 5, p. 5754, https://doi.org/10.1038/ncomms6754.

Shields, G.A., 2018, Carbon and carbon isotope mass balance in the Neoproterozoic Earth system: Emerging Topics in Life Sciences, v. 2, p. 257–265, https://doi.org/10.1042/ETLS20170170.

Siever, R., 1992, The silica cycle in the Precambrian: Geochimica et Cosmochimica Acta, v. 56, p. 3265–3272, https://doi.org/10.1016/0016-7037(92)90303-Z.

Stolper, D.A., Love, G.D., Bates, S., Lyons, T.W., Young, E., Sessions, A.L., and Grotzinger, J.P., 2017, Paleoecology and paleoceanography of the Athel silicilyte, Ediacaran-Cambrian boundary: Sultanate of Oman: Geobiology, v. 15, p. 401–426, https://doi.org/10.1111/gbi.12236.

Tarhan, L.G., Hood, A.S., Droser, M.L., Gehling, J.G., and Briggs, D.E., 2016, Exceptional preservation of soft-bodied Ediacara biota promoted by silica-rich oceans: Geology, v. 44, p. 951–954, https://doi.org/10.1130/G38542.1.

Tarhan, L.G., Droser, M.L., Gehling, J.G., and Dzaugis, M.P., 2017, Microbial mat sandwiches and other anactualistic sedimentary features of the Ediacara Member (Rawnsley Quartzite, South Australia): Implications for interpretation of the Ediacaran sedimentary record: Palaios, v. 32, p. 181–194, https://doi.org/10.2110/palo.2016.060.

Tarhan, L.G., Planavsky, N.J., Wang, X., Bellefroid, E.J., Droser, M.L., and Gehling, J.G., 2018, The late-stage "ferruginization" of the Ediacara Member (Rawnsley Quartzite, South Australia): Insights from uranium isotopes: Geobiology, v. 16, p. 35–48, https://doi.org/10.1111/gbi.12262.

Wilkin, R.T., and Barnes, H.L., 1997, Formation processes of framboidal pyrite: Geochimica et Cosmochimica Acta, v. 61, p. 323–339, https://doi.org/10.1016/S0016-7037(96)00320-1.

Printed in USA